

Cellular Shade Energy Savings in a Commercial Setting



Mahabir Bhandari
Niraj Kunwar
Anthony Gehl
Stephen Mullaly
Stacy Lambright

December 2022

FINAL CRADA REPORT
CRADA NO. NFE-21-08440



DOCUMENT AVAILABILITY

Reports produced after January 1, 1996, are generally available free via OSTI.GOV.

Website www.osti.gov

Reports produced before January 1, 1996, may be purchased by members of the public from the following source:

National Technical Information Service
5285 Port Royal Road
Springfield, VA 22161
Telephone 703-605-6000 (1-800-553-6847)
TDD 703-487-4639
Fax 703-605-6900
E-mail info@ntis.gov
Website <http://classic.ntis.gov/>

Reports are available to US Department of Energy (DOE) employees, DOE contractors, Energy Technology Data Exchange representatives, and International Nuclear Information System representatives from the following source:

Office of Scientific and Technical Information
PO Box 62
Oak Ridge, TN 37831
Telephone 865-576-8401
Fax 865-576-5728
E-mail reports@osti.gov
Website <https://www.osti.gov/>

This report was prepared as an account of work sponsored by an agency of the United States Government. Neither the United States Government nor any agency thereof, nor any of their employees, makes any warranty, express or implied, or assumes any legal liability or responsibility for the accuracy, completeness, or usefulness of any information, apparatus, product, or process disclosed, or represents that its use would not infringe privately owned rights. Reference herein to any specific commercial product, process, or service by trade name, trademark, manufacturer, or otherwise, does not necessarily constitute or imply its endorsement, recommendation, or favoring by the United States Government or any agency thereof. The views and opinions of authors expressed herein do not necessarily state or reflect those of the United States Government or any agency thereof.

Buildings and Transportation Science Division

CELLULAR SHADE ENERGY SAVINGS IN A COMMERCIAL SETTING

Mahabir Bhandari
Niraj Kunwar
Anthony Gehl
Stephen Mullaly*
Stacy Lambright*

*Hunter Douglas N. V.

December 2022

Prepared by
OAK RIDGE NATIONAL LABORATORY
Oak Ridge, TN 37831
managed by
UT-BATTELLE LLC
for the
US DEPARTMENT OF ENERGY
under contract DE-AC05-00OR22725

CONTENTS

LIST OF FIGURES	v
LIST OF TABLES	vi
ACKNOWLEDGEMENTS	vii
ABSTRACT.....	viii
1. INTRODUCTION	1
2. METHODOLOGY	1
2.1 EXPERIMENTAL TESTING	1
2.1.1 Experimental Facility and Test Rooms	1
2.1.2 Shading Device and Sensor Instrumentation	3
2.1.3 Test Cases and Shade Operation Schedule	5
2.2 FRP MODEL CALIBRATION	6
2.2.1 Baseline Summer	7
2.2.2 Shaded Summer	8
2.3 PROTOTYPE BUILDING SIMULATION	9
3. RESULTS	9
3.1 EXPERIMENTAL TESTING	9
3.1.1 Energy Consumption and Savings	9
3.1.2 Thermal Comfort	12
3.1.3 Daylighting and Visual Comfort.....	14
3.2 ANNUAL SIMULATION.....	19
4. CONCLUSIONS	21
5. REFERENCES	23

LIST OF FIGURES

Figure 1. FRP building at ORNL (four rooms used for the experiment labeled).	2
Figure 2. Floor plan of the first floor of the FRP building with two rooms (room 104 and room 106) used for experimental testing.	3
Figure 3. D22 Duette Commercial FR with MicroShield 3/4 in. single cell.....	4
Figure 4. Test room with cellular shades in the closed position in two windows and illuminance sensors.....	4
Figure 5. Floor plan of the rooms with locations of WPI sensors and VI sensors.	5
Figure 6. Geometry for the energy model of the FRP building.	6
Figure 7. Cooling load for room 204 from measured and simulated data for BS.	7
Figure 8. Room temperature for room 204 from measured and simulated data for BS.	7
Figure 9. Cooling load in room 204 from measured and simulated data (using Simple window model and BSDF model) for SS.	8
Figure 10. Room temperature in room 204 from measured and simulated data (using Simple window model and BSDF model) for SS.....	9
Figure 11. Boxplot distributions of daily cooling energy for BS and SS for four rooms.	10
Figure 12. Boxplot distributions of daily heating energy for BW and SW for four rooms.	11
Figure 13. Heating and cooling energy with dry bulb temperature (DBT) in room 104 for BW.	12
Figure 14. Temperature in the gap between the glass and shade for three cases (BW, SW, and SS) for room 206, and temperature at the same location without any shades for room 106.	13
Figure 15. MRT at a sensor at a distance of 0.6 m from the window in the south orientation for three cases (BW, SW, and SS) in rooms 106 and 206.	14
Figure 16. UDI at four different sensor locations for BD (all the windows are without any shading devices).	15
Figure 17. UDI at four different sensor locations for SS.	16
Figure 18. Illuminance at sensor A1 for BD and SS in rooms (a) 106 and 206 and (b) 104 and 204.	17
Figure 19. DGPs at two sensors for BD.....	18
Figure 20. DGPs at two sensors for SS.....	18
Figure 21. EUI for cooling for six cases and three locations.	19
Figure 22. EUI for heating for six cases and three locations.	20
Figure 23. HVAC savings relative to baseline case for six cases and three locations.	21

LIST OF TABLES

Table 1. Location and orientation of the rooms used for experimental testing.....	3
Table 2. Test cases for experimental testing	6
Table 3. Schedule of opening and closing of shades	6
Table 4. Cooling energy consumption and savings during summer/cooling season test (BS and SS).....	10
Table 5. Heating energy consumption and savings during winter/heating season test (BW and SW).....	12
Table 6. Cooling energy consumption and savings during winter/heating season test (BW and SW).....	12

ACKNOWLEDGEMENTS

We would like to thank Hunter Douglas for providing the cellular shades for the experimental testing. We would also like to thank Piljae Im, Sungkyun Jung, and Yeobeom Yoon for the energy model of the Flexible Research Platform (FRP) building and for feedback on the energy model calibration.

This work is supported by the Buildings Technology Office of the US Department of Energy, and we specifically thank Marc LaFrance at the US Department of Energy for guiding this research.

ABSTRACT

Windows cause approximately 1.7 quad of heating and cooling energy consumption in the United States. This energy consumption can be reduced by using high-efficiency window attachments. Common Venetian blinds and planar shades, such as roller shades, might block solar radiation, but they do not provide a significant improvement to window system thermal transmittance. Cellular shades have better thermal performance compared to other shading devices because of the honeycomb structure that traps air in pockets to create thermal insulation. However, evaluating the energy savings potential of cellular shades using experimental testing in commercial settings is limited. Moreover, the effect of cellular shades on daylighting and glare is yet to be evaluated using field testing. In this study, experimental testing of cellular shades was performed in a real building with emulated occupancy for both a cooling and a heating season. Compared with a room without shades, the use of cellular shades in experimental testing showed incremental energy savings of 4.6% to 9.4% for cooling and higher than 20% for heating. The experimental data were used to calibrate the baseline energy model and validate the cellular shades model. Annual simulation of cellular shades was performed for a medium office prototype building using the validated cellular shades model. The annual simulation was performed in Phoenix, Nashville, and Rochester. The annual savings for HVAC energy was 25% for Phoenix, 27% for Nashville, and 19% for Rochester.

1. INTRODUCTION

Windows cause approximately 1.7 quad of heating and cooling energy consumption in the United States. A study conducted by Pacific Northwest National Laboratory showed that the installation of a high-efficiency window attachment, such as cellular shades, is estimated to reduce HVAC energy consumption up to 25% in residential single-family homes during the cooling season [1]. Venetian blinds and planar shades, such as roller shades, might block solar heat gain, but they do not provide significant improvement to window system thermal transmittance [2]. Cellular shades have better thermal performance compared with other shading devices because of the honeycomb structure that traps air inside pockets and creates thermal insulation. However, the adoption of cellular shades is very low compared to blinds and curtains, which comprise 60% and 19%, respectively, of all the window coverings in the United States [3].

The number of studies on cellular shades is also limited compared with other shading devices. Hart performed experimental testing of cellular shades in a laboratory environment using 13 cellular shades [4]. Hart's study validated the heat flux simulated by WINDOW [5] against measured data but did not measure or validate the solar heat gain. A parametric energy simulation study of shade properties, including cellular shades, was performed to evaluate their impact on air-conditioning in residential buildings [6]. A previous experimental study conducted by the authors of the present study showed cellular shades achieve daily energy savings in the range of 17%–36% during the heating season compared with the case without shades [7]. However, experimental testing of cellular shades in commercial buildings for their energy savings potential is lacking. In commercial buildings, cellular shades are also important for maintaining appropriate daylighting and occupant comfort in the space in addition to the energy savings and demand reduction potential. In this study, the team investigated the energy and daylighting effect of light-filtering cellular shades using an experiment and building energy simulation.

2. METHODOLOGY

This section discusses the experimental testing and energy simulations performed for cellular shades. First, experimental testing was done in a facility located at Oak Ridge National Laboratory (ORNL), which is discussed in the following section. Then, this study provides a description of energy model development and calibration for the facility. Finally, energy simulation based on the validated shade model used on a medium office reference building is used to evaluate the effect of cellular shades on building levels in three locations throughout the United States.

2.1 EXPERIMENTAL TESTING

2.1.1 Experimental Facility and Test Rooms

The experimental testing was performed in the Flexible Research Platform (FRP) building at ORNL. The FRP building is a two-story building representative of a small office building with a total floor area of 3,872 ft² (1,936 ft²/floor). The FRP building is instrumented to measure the indoor environment and delivered energy for each of the rooms, as well as collect weather data at the building site. In this study, four rooms were used to evaluate the energy and daylighting effect of the cellular shades. A picture of the FRP building with labels for the four rooms used (104, 106, 204, and 206) for the experimental testing is shown in Figure 1.



Figure 1. FRP building at ORNL (four rooms used for the experiment labeled).

A floor plan of the first floor of the building is shown in Figure 2, along with two of the rooms used for the experimental testing. Two of the four test rooms (104 and 204) had north- and west-facing windows, and the other two (106 and 206) had east- and south-facing windows. All four rooms were identical in size. The main objective of using the test rooms on different floors was to perform parallel testing between the rooms on two floors to see the effect of cellular shades when the two rooms on different floors were exposed to the same weather conditions. The floor where each room is located and the orientation of exterior windows are listed in Table 1.

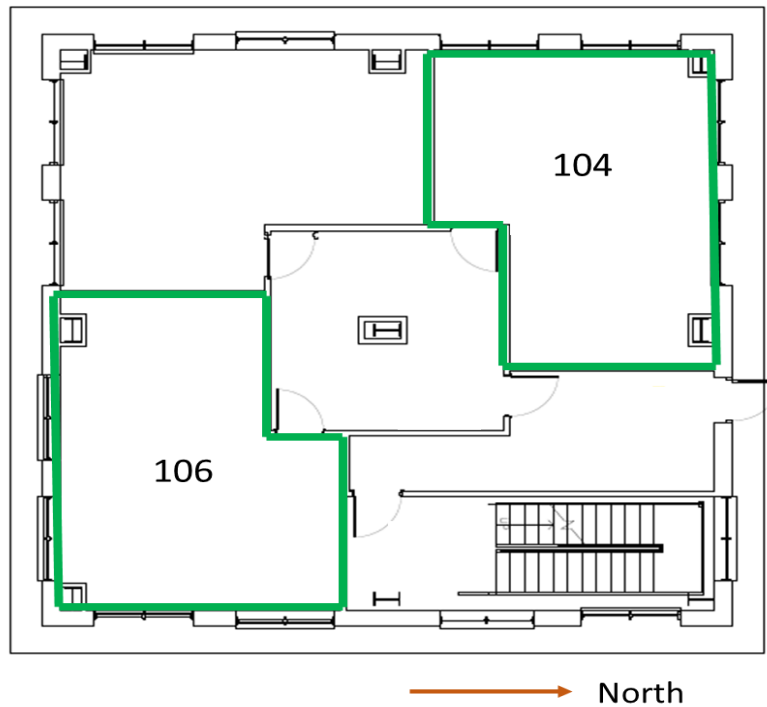


Figure 2. Floor plan of the first floor of the FRP building with two rooms (room 104 and room 106) used for experimental testing.

Table 1. Location and orientation of the rooms used for experimental testing

Room	Floor	Orientation
104	1	North and west (NW)
204	2	North and west (NW)
106	1	South and east (SE)
206	2	South and east (SE)

2.1.2 Shading Device and Sensor Instrumentation

This study used a light-filtering single cell-type cellular shade (Hunter Douglas Duette Commercial Flame-Resistant [FR] with MicroShield 3/4 in. Honeycomb Shade [D22]), shown in Figure 3. Light-filtering shades allow natural daylight through the window even when the shades are closed, providing energy savings and daylight at the same time. Figure 4 shows cellular shades installed in a test room, along with some illuminance sensors. Figure 5 shows the layout of the work plane illuminance (WPI) sensor and vertical illuminance (VI) sensors for the four rooms used in the experiment. Each room had a similar setup of the illuminance sensors, with four sensors used for daylight evaluation and two sensors used for glare evaluation. The WPI sensors were placed at 1 m and 3 m distances from the south window in 106 and 206, and at the same distances from the north window in 104 and 204 respectively. All WPI sensors were facing the ceiling and were at a height of 0.76 m. The VI sensors were placed at a distance of 1.5 m from the window at a height of 1.2 m from the ground facing the window. Thus, the VI sensors were placed facing the south and east windows in 106 and 206, and they were facing the west and north windows in 104 and 204.



Figure 3. D22 Duette Commercial FR with MicroShield 3/4 in. single cell.



Figure 4. Test room with cellular shades in the closed position in two windows and illuminance sensors.

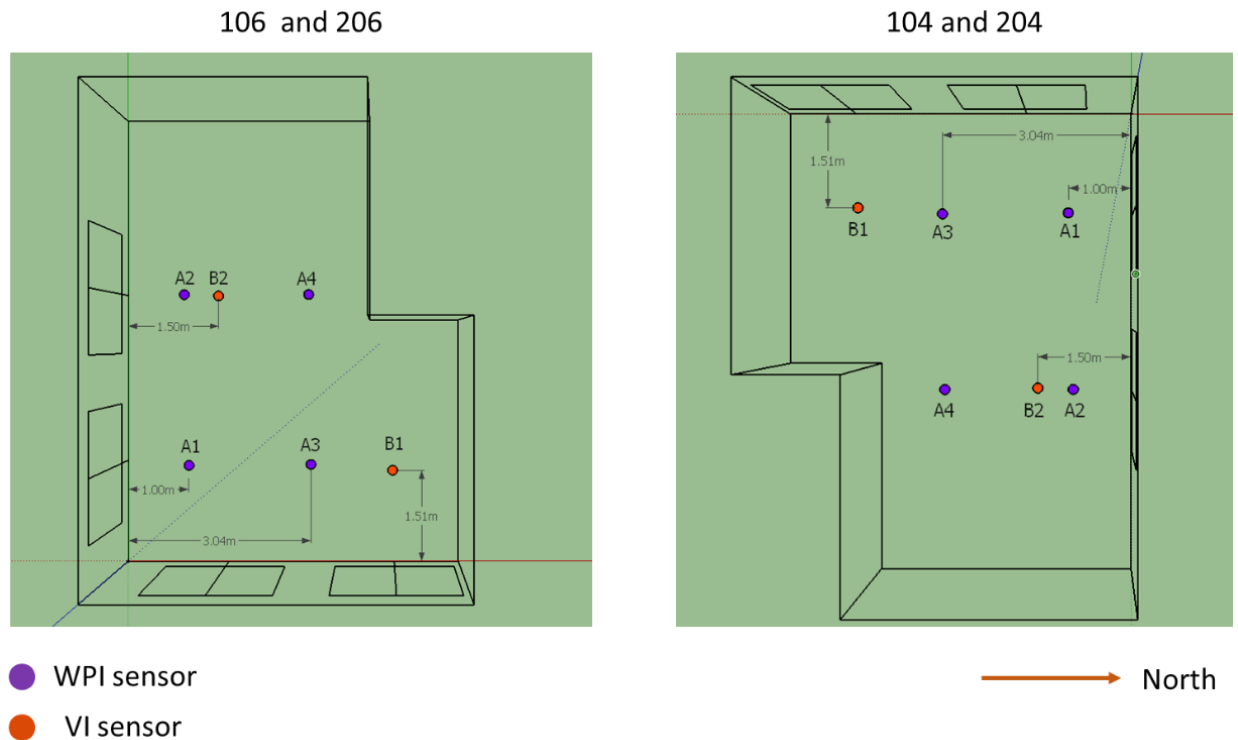


Figure 5. Floor plan of the rooms with locations of WPI sensors and VI sensors.

The data were collected for weather, room temperature, supply air temperature, supply air flow rate, WPI, VI, and return air temperature for each of the rooms. From the data collected, the delivered heating and cooling energy for each of the rooms was calculated. In addition to these sensors, surface temperature sensors were installed in the windows, and temperature sensors were installed in the gap between the window and the cellular shades. Also, mean radiant temperature (MRT) sensors were installed after the location of cellular shades in the south and north orientation.

2.1.3 Test Cases and Shade Operation Schedule

Table 2 shows the cases that were tested during the experiment. These cases varied based on the setting of the cellular shades, the season for the testing, and the objective of the experimental testing. The test duration in Table 2 is the number of testing days after filtering out data from days where the testing was not valid because of faulty HVAC operation. The operation of the shade in the room with D22 (listed in Table 2) was based on season and orientation. The operation of shades during different seasons for different orientations are listed in Table 3. During summer, the shades in all the orientations were closed (deployed) for 24 h/day to block unwanted solar heat gains. During winter, the shades were open from 8 A.M. to 12 P.M. in the east orientation, 8 A.M. to 4 P.M. in the south orientation, and 12 P.M. to 4 P.M. in the west orientation. The shades were open during these hours so that solar heat could be harvested in each orientation when sunlight was falling in the orientation. In the north orientation, the shades were closed at all hours. The time period of opening and closing a shade was scheduled with the objective of energy efficiency for a generic building located in the northern hemisphere.

Table 2. Test cases for experimental testing

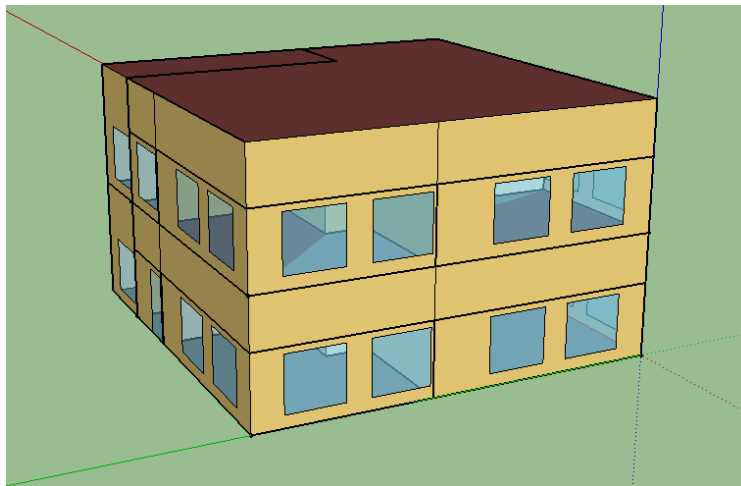
Test case	Shade (104 and 106)	Shade (204 and 206)	Test duration (days)
Baseline winter (BW)	—	—	5
Shaded winter (SW)	—	Single-cell honeycomb shade (D22)	5
Baseline summer (BS)	—	—	6
Shaded summer (SS)	—	Single-cell honeycomb shade (D22)	7
Baseline daylight (BD)	—	—	6

Table 3. Schedule of opening and closing of shades

Orientation	Winter schedule	Summer schedule
North	Always closed	Always closed
East	Open: 8 A.M.–12 P.M.	Always closed
South	Open 8 A.M.–4 P.M.	Always closed
West	Open 12 P.M.–4 P.M.	Always closed

2.2 FRP MODEL CALIBRATION

The energy model was created for the FRP building using EnergyPlus [8]. The geometry of the whole building energy model is shown in Figure 6. The building had a total of 10 conditioned zones, among which this study was interested in four zones, where experimental tests were conducted. Cooling for each zone was provided by a combination of cooling air provided by a rooftop unit (RTU) that was controlled before reaching a zone by a variable air volume (VAV) box terminal for each of the zones. The RTU had a total cooling capacity of 39 kW with a coefficient of performance of 3.22. The heating for each zone was provided by reheat electricity at the VAV box terminal for each of the zones.

**Figure 6. Geometry for the energy model of the FRP building.**

The energy model was created using available information on building construction and operation, such as heating and cooling set point, measured plug loads and lighting loads. The uncertainty resulting from

occupants in a building was not present because the building was unoccupied. The load from the occupancy was emulated using a heater for plug loads and a humidifier for the latent load from occupants. The model calibration was performed for one room (204) for a baseline window using the experimental data from Baseline Summer (BS). Next, model validation was performed for the model of the cellular shades added to the calibrated baseline model using experimental data from Shaded Summer (SS). Two different models in EnergyPlus were compared against the experimental data for model validation. The similarity between the measured and the simulated cooling loads was evaluated using the metrics mean bias error (MBE) and coefficient of variation of root mean square error (CV-RMSE) following ASHRAE Guideline 14 [9]. According to ASHRAE Guideline 14, the models are calibrated for energy use if the MBE is within $\pm 10\%$ and CV-RMSE is within 30% when using hourly data. The results from the model calibration for room 204 during BS and SS are discussed in the next sections.

2.2.1 Baseline Summer

The comparison between the measured and simulated data for cooling energies (cooling loads) for BS is provided in Figure 7 and room temperatures for BS in Figure 8. For hourly data, the MBE for cooling energy was 4.8%, and the CV-RMSE was 27%; both values were within the limit specified for model calibration.

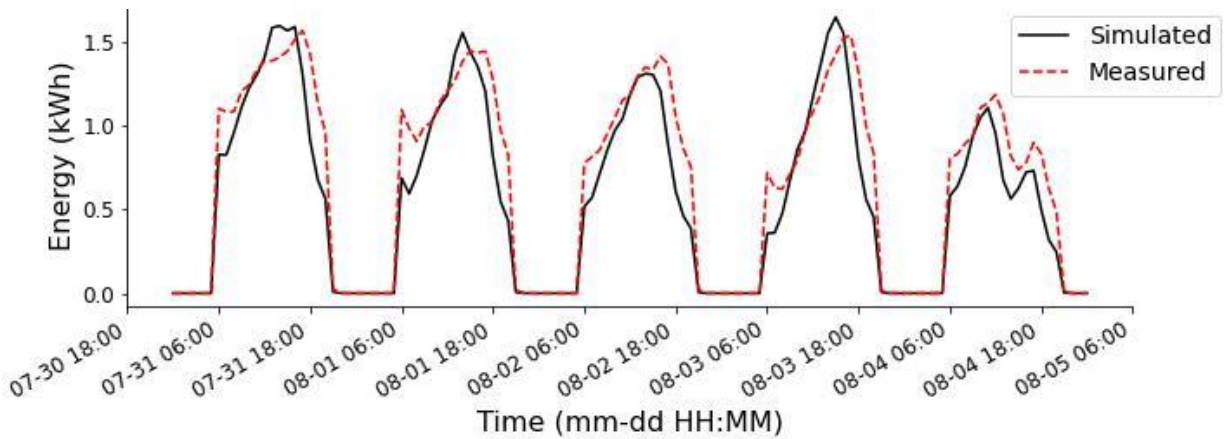


Figure 7. Cooling load for room 204 from measured and simulated data for BS.

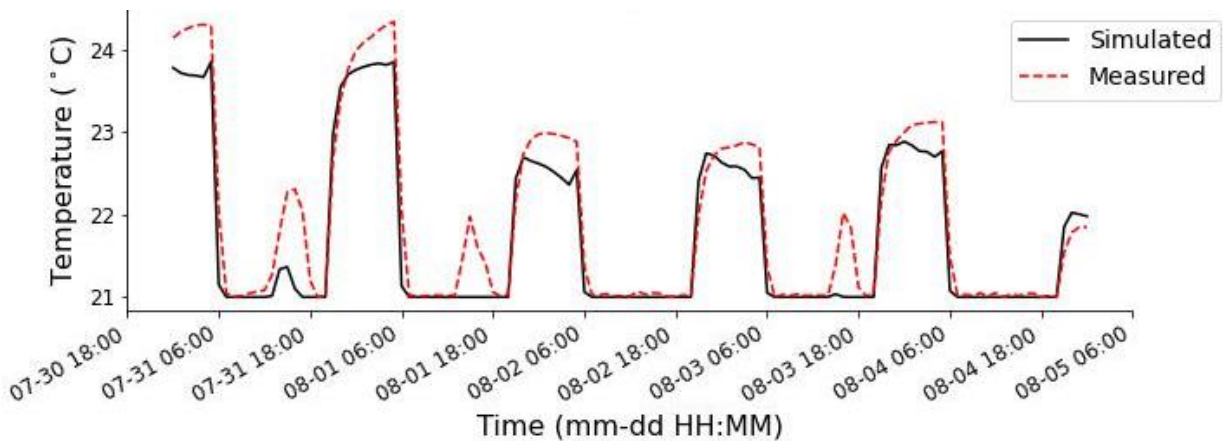


Figure 8. Room temperature for room 204 from measured and simulated data for BS.

2.2.2 Shaded Summer

The comparison between the measured and simulated cooling energies and room temperatures for SS is provided in Figure 9 and Figure 10, respectively. For the SS model, cellular shades were added to room 204 in the calibrated model discussed in Section 2.2.1. The combination of windows and shading devices (cellular shades in this study) is also called a *complex fenestration system*. Two models for the complex fenestration system were used in this study. One of the models was called the *Simple* model, which used only window thermal transmittance (U-factor), solar heat gain coefficient, and visible transmittance as input. The second model, using a function called the *bidirectional scattering distribution function* (BSDF), was also used for the energy simulation and was generated using WINDOW [5]. The input for the Simple model was based on the U-factor, solar heat gain coefficient, and visible transmittance calculated in WINDOW using the BSDF model.

The BSDF model is supposed to be more accurate when compared with the Simple model because BSDF can account for the effect of solar angle as well as direct and diffuse contribution for the solar gain. However, this accuracy does not seem to be the case in Figure 9, where the cooling energy from using the Simple model is closer to measured data compared with the BSDF model. MBE and CV-RMSE between the measured and simulated cooling load for the BSDF model, MBE was 30.6%, and CV-RMSE was 47.4%. MBE was 9.3% and CV-RMSE was 21.2% for the Simple model. The BSDF model seems to underpredict the cooling load. This phenomenon was also seen in a study by Kunwar et. al., where the BSDF model underpredicted the cooling load compared with measured data and another model that used simple properties for each layer of window [7]. Next, the Simple model was used to calculate the energy savings potential at the building level, as discussed in Section 2.3.

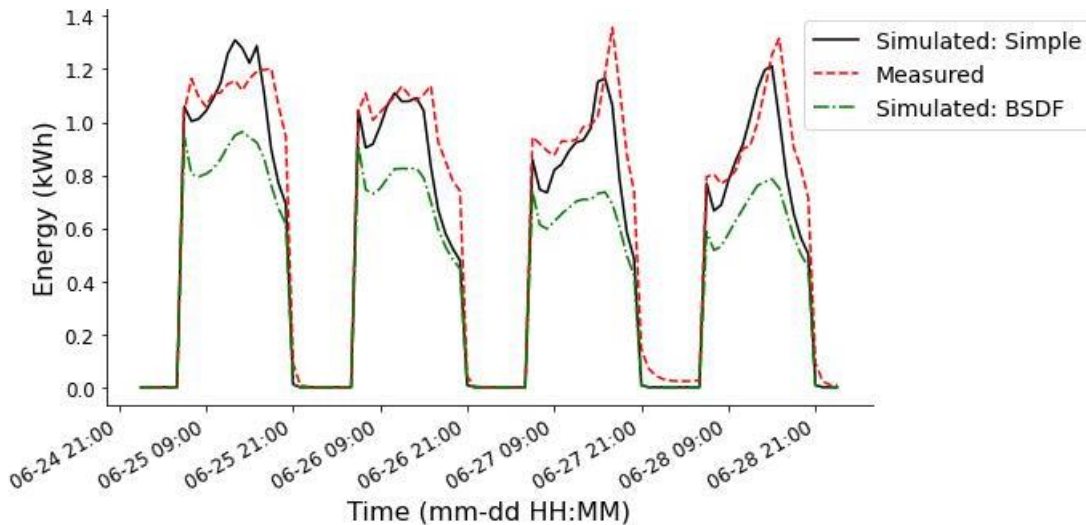


Figure 9. Cooling load in room 204 from measured and simulated data (using Simple window model and BSDF model) for SS.

For room temperature, Figure 10 shows that both the Simple and BSDF models are very close to each other and reasonably capture the measured room temperature in the energy model.

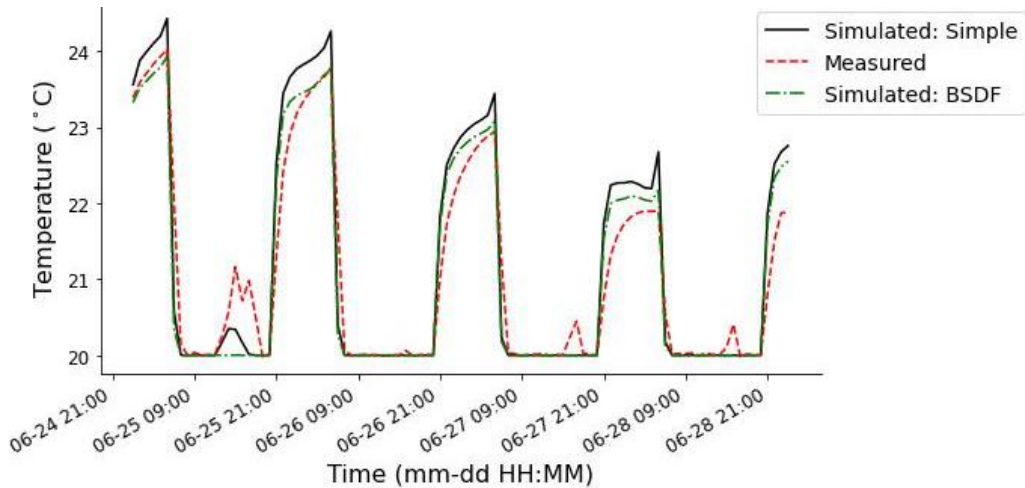


Figure 10. Room temperature in room 204 from measured and simulated data (using Simple window model and BSDF model) for SS.

2.3 PROTOTYPE BUILDING SIMULATION

Annual simulations were performed using a medium office prototype building developed by the US Department of Energy [10]. The building had a gross wall area of 21,398 ft² with a window-to-wall ratio of 33% (6,921 ft²). The building had three packaged air-conditioning units with a multizone variable air volume system using a gas furnace and electric reheat for heating. The cooling coil on each of the air-conditioning units was a two-speed coil with a gross rated coefficient of performance of 2.8 at high speed and 2.84 at low speed. The burner efficiency for the gas furnace was 0.8. The window glazing of the prototype building was converted to double-clear glazing for the baseline case. Energy simulations were performed at three locations of Phoenix (AZ), Nashville (TN), and Rochester (NY). Phoenix, Nashville, and Rochester represent a hot climate (climate zone 2A), a moderate climate similar to physical testing (climate zone 3A), and a cold climate (climate zone 6A) respectively. For each of these locations following cases were used for energy simulation.

- Baseline: Double clear glazing
- Low-e: Double Low-E glazing
- Blinds: Interior venetian blinds installed on double clear glazing which was closed all the time
- Shades: Interior roller shades installed on double clear glazing which was closed all the time
- D22: D22 cellular shades installed on the baseline window
- D22 Low-e: D22 cellular shades installed on the Low-e window

3. RESULTS

3.1 EXPERIMENTAL TESTING

3.1.1 Energy Consumption and Savings

The energy consumption of each of the four rooms used for experimental testing is evaluated in terms of delivered heating and cooling energy. The energy consumption was compared for two rooms in the same orientation (i.e., 106 vs. 206 and 104 vs. 204). This comparison was performed for two cases: (1) without any shading devices in both rooms and (2) with shading devices in one of the two rooms for summer (cooling) and winter (heating) seasons.

3.1.1.1 Summer/Cooling Season Energy Savings

Figure 11 shows the distribution of daily cooling energy for BS and SS for all four rooms. For BS, none of the rooms used any shades. For SS (as noted in Table 1), rooms 204 and 206 on the second floor used cellular shades, and rooms 104 and 106 were without any shades. Rooms 106 and 206 had similar energy consumption for BS. The mean energy consumption of 204 was lower than 104, showing that rooms 104 and 204 already had different cooling energy when both rooms had no shades. This difference should be adjusted when evaluating the energy savings from using cellular shades in 204. In rooms 106 and 206, the difference between the energy consumption in SS was representative of energy savings because the energy consumption was similar for BS when both rooms had no shades.

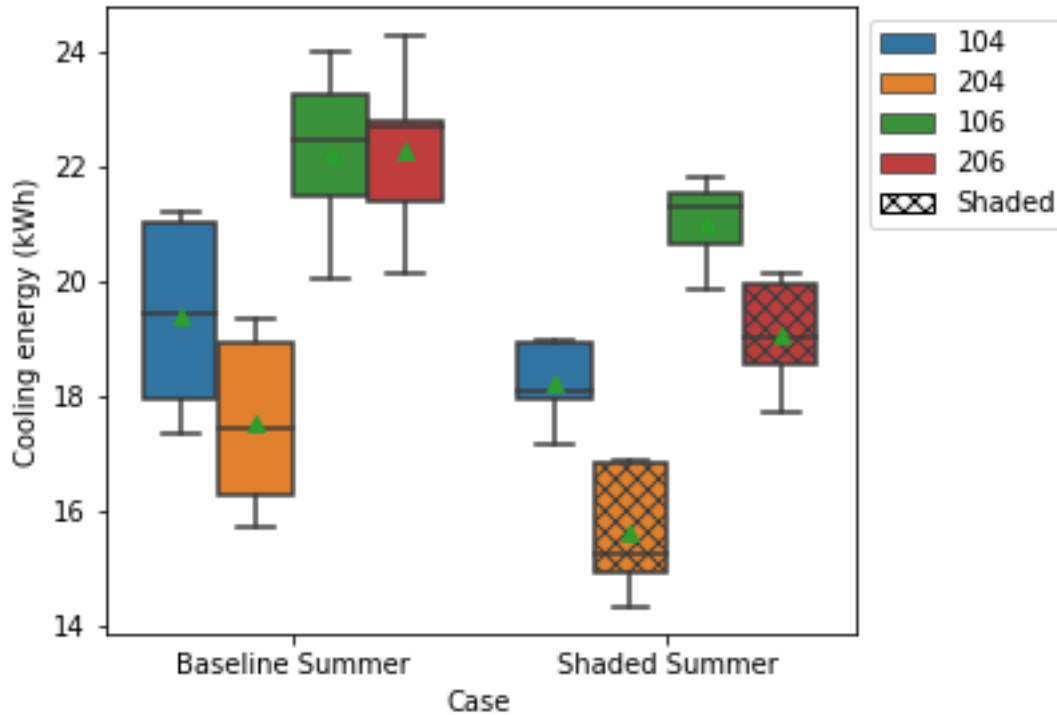


Figure 11. Boxplot distributions of daily cooling energy for BS and SS for four rooms. The green triangle marker represents the mean value of the distribution.

Table 4 provides the average daily energy consumption and percentage savings, which is the difference in energy of room 204 from 104 and 206 from 106. During the cooling season, no heating energy was delivered, so only results for cooling energy demand are provided. The incremental energy savings at rooms in the north and west orientation (104 and 204) was 4.6% when adjusted for room variations, and the south and east orientation rooms (106 and 206) was 9.3%. The higher energy savings in the south and east-oriented rooms might be because, in the south orientation, solar radiation falls on the window for a longer duration, thus providing the cellular shades the potential to block more solar heat gain.

Table 4. Cooling energy consumption and savings during summer/cooling season test (BS and SS)

Case	Cooling energy (kWh)		Savings (%)	Cooling energy (kWh)		Savings (%)
	104	204		106	206	
BS	19.4	17.6	9.6	22.3	22.3	0.0
SS	18.2	15.6	14.2	21.1	19.1	9.3

3.1.1.2 Winter/Heating Season Energy Savings

The box plot distribution for the heating energy consumption for the four rooms for BW and SW is provided in Figure 12. The figure shows that even for BW, the difference in heating energy for rooms 106 and 206 was higher compared with the difference between heating energy for rooms 104 and 204. After using the shading device in 204 and 206, the energy consumption was lowered compared with 104 and 106. The average daily heating energy consumption and percentage energy savings are provided in Table 5. The percentage energy savings were calculated based on the difference in heating energy of rooms 204 and 104 and rooms 206 from 106, similar to the calculation for the cooling season. The results show that when no shade is present in all 4 rooms, in the north and west orientation, the difference in heating was 21.7%, and in the south and east orientation, the difference was 68.2%. This difference increased to 78.8% in the north and west orientation and 92.2% in the south and east orientation for Shaded Winter (SW) after using cellular shades in rooms 204 and 206. This huge difference in energy savings occurred because some heating to the rooms is provided by a heater, which is used as the plug load in the room and is not included in the heating energy in Figure 12. Another notable occurrence during the heating season was the presence of significant cooling energy consumption. The cooling energy consumption and differences in energy consumption between rooms 104 and 204 and rooms 106 and 206 for the heating season are provided in Table 6. The cooling energy demand occurred during the afternoon hours owing to a combination of internal load and solar heat gain. An example of cooling energy during the heating season along with outdoor dry bulb temperature (DBT) is shown in Figure 13 for room 106 for three days of BW. The heating energy consumption occurred during morning and evening hours, and the cooling energy consumption occurred during midday.

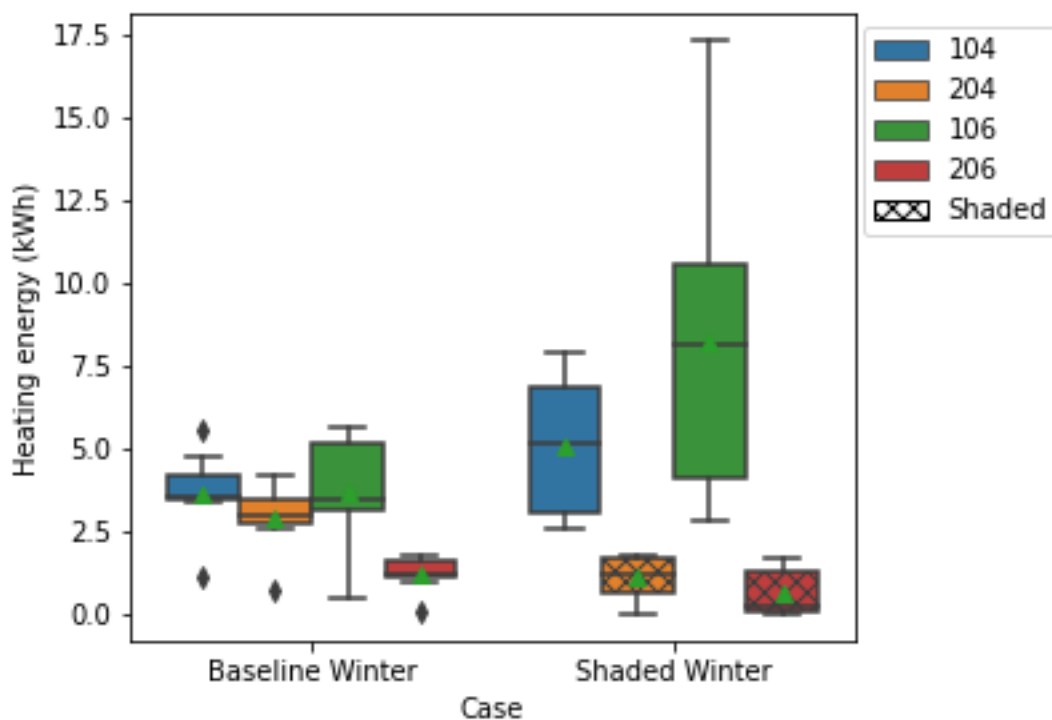


Figure 12. Boxplot distributions of daily heating energy for BW and SW for four rooms. The green triangle marker represents the mean value of the distribution.

Table 5. Heating energy consumption and savings during winter/heating season test (BW and SW)

Case	Heating energy (kWh)		Savings (%)	Heating energy (kWh)		Savings (%)
	104	204		106	206	
BW	3.6	2.9	21.7	3.7	1.2	68.2
SW	5.0	1.1	78.8	8.2	0.6	92.2

Table 6. Cooling energy consumption and savings during winter/heating season test (BW and SW)

Case	Cooling energy (kWh)		Savings (%)	Cooling energy (kWh)		Savings (%)
	104	204		106	206	
BW	3.1	3.8	-22.1	9.7	12.1	-24.9
SW	2.9	4.6	-58.3	7.5	11.5	-52.5

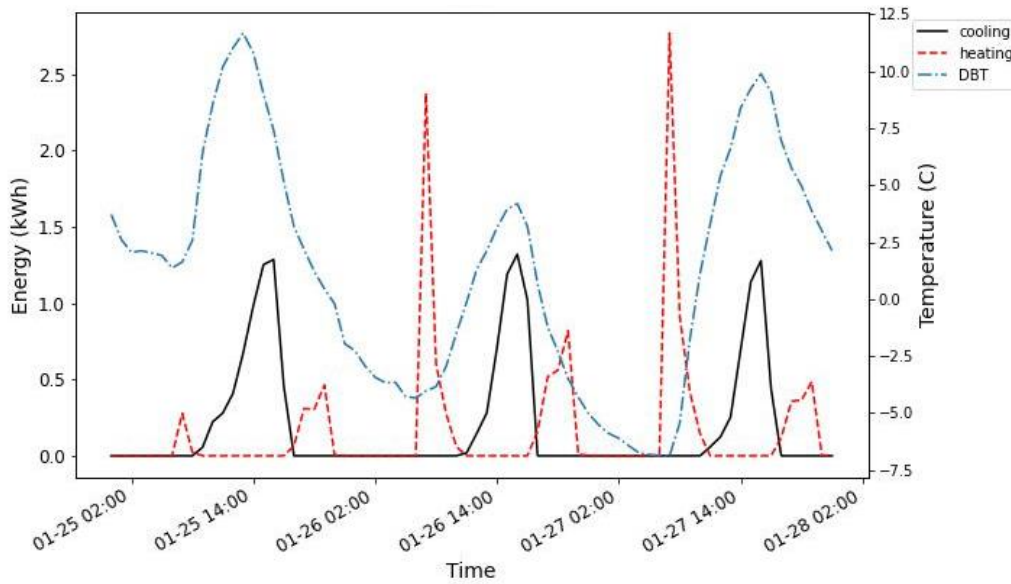


Figure 13. Heating and cooling energy with dry bulb temperature (DBT) in room 104 for BW.

3.1.2 Thermal Comfort

Data from temperature sensors in the gap between windows and shades and MRT sensors were used to evaluate how cellular shades affect the heat transfer through the window and its potential impact on thermal comfort. Figure 14 shows the temperature at the gap between the window and cellular shades (gap temperature) in the south orientation for room 206 and the temperature at a similar location for room 106, which did not have any shades. For BW, the gap temperature in 206 was slightly higher than 106 during afternoon hours and similar at other times. For SW, the gap temperatures at 206 and 106 follow a similar trend as BW. One of the reasons for this similarity might be that the shades were open during the winter testing at the south orientation from 8 A.M. to 4 P.M. A significant difference in the gap temperature between 106 and 206 was seen for SS. In this case, the cellular shades at 206 were always closed, which trapped the heat gain from the window in the gap between the window and the cellular shades. The effect of this phenomenon on the MRT at a distance of 0.6 m from the window is shown in Figure 15. Here, the MRT at BW and SW had a similar trend for rooms 106 and 206. However, the difference in MRT between 106 and 206 was significant for SS. In room 206, during the occupied hours

of 7 A.M. to 10 P.M., the MRT was always below 24°C, and it was above 26°C for 106. Therefore, it can be observed that using cellular shades can help to maintain thermal comfort near the room set point temperature (23.88°C) compared to a room without any shades.

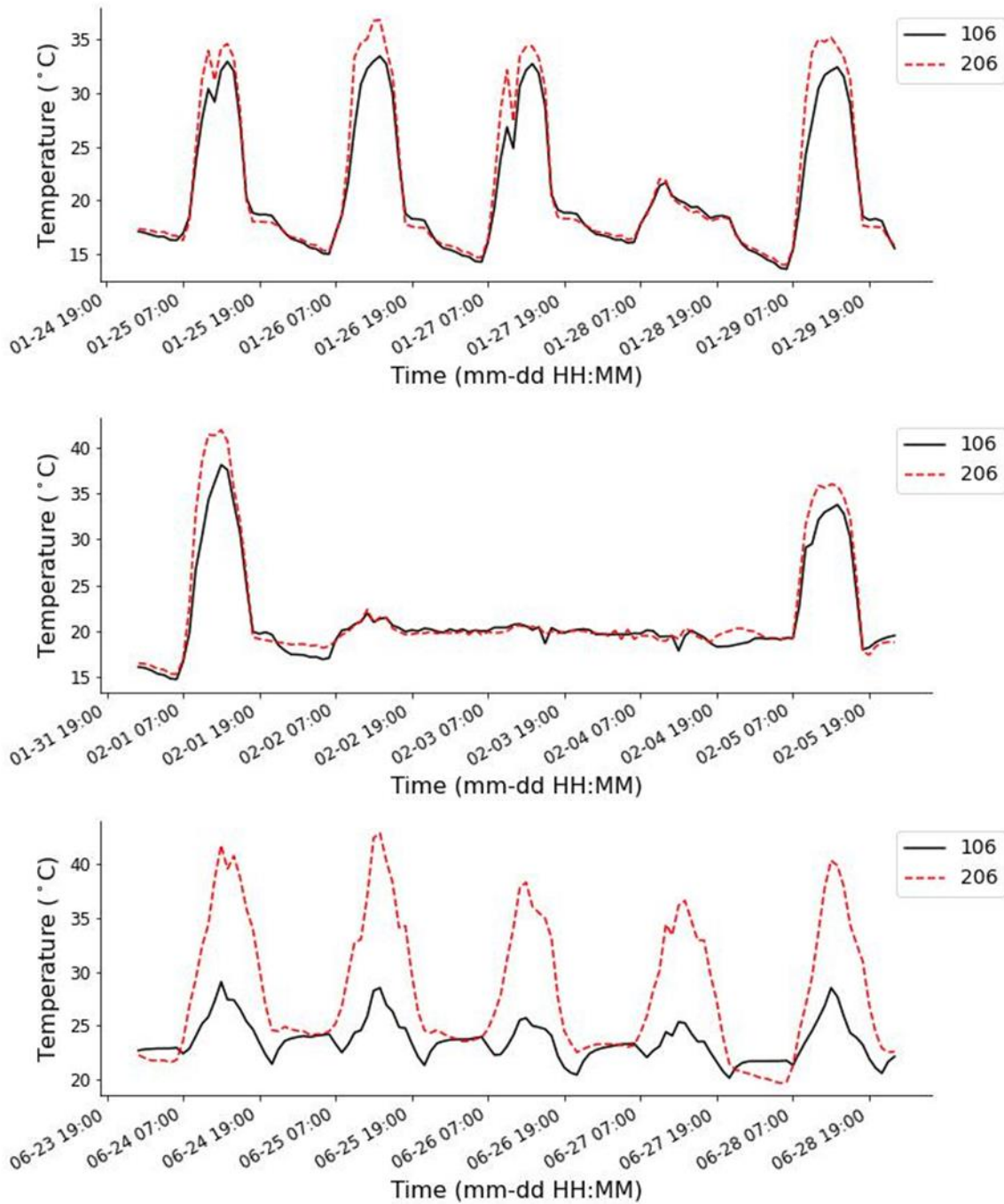


Figure 14. Temperature in the gap between the glass and shade for three cases (BW, SW, and SS) for room 206, and temperature at the same location without any shades for room 106.

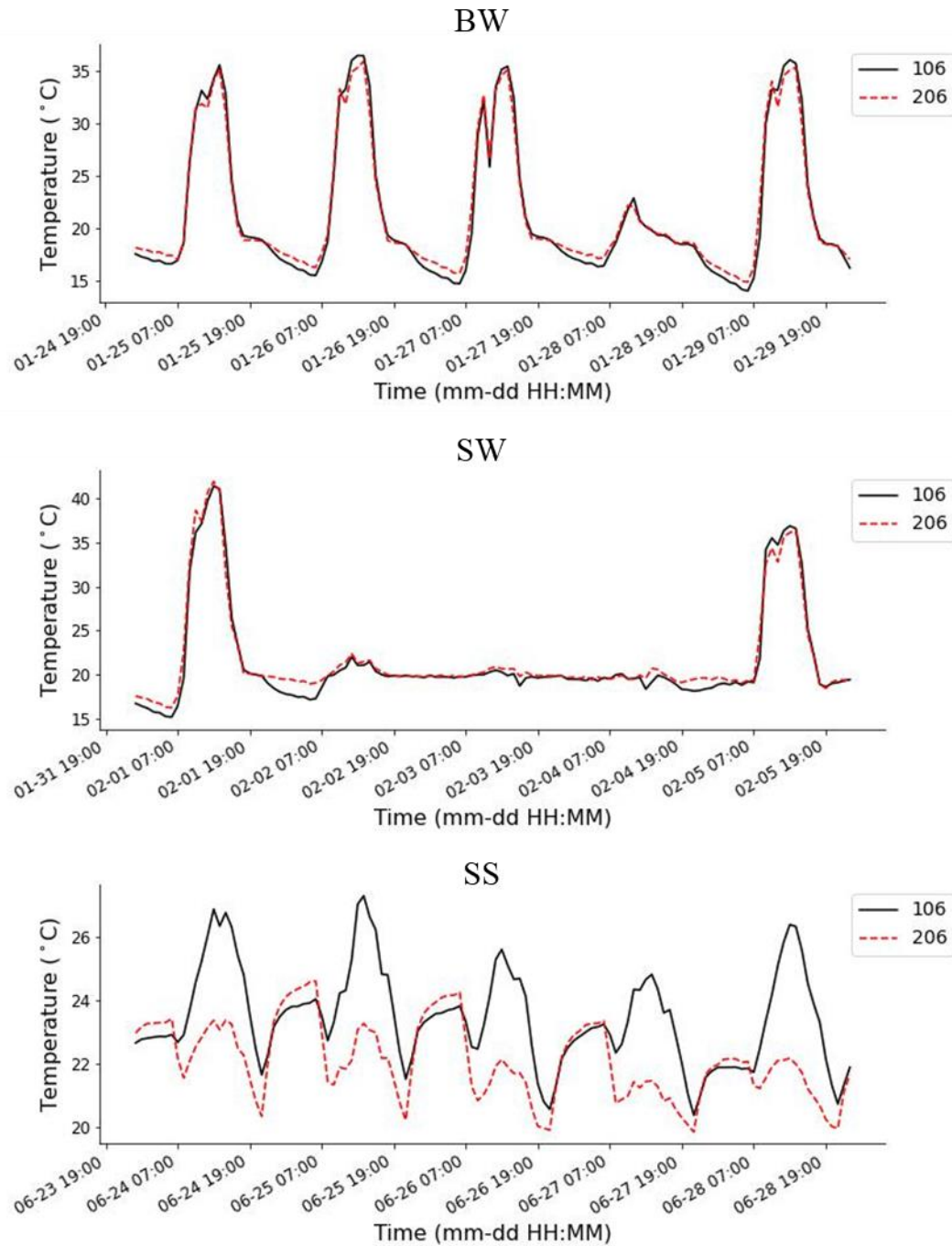


Figure 15. MRT at a sensor at a distance of 0.6 m from the window in the south orientation for three cases (BW, SW, and SS) in rooms 106 and 206.

3.1.3 Daylighting and Visual Comfort

Daylighting and visual comfort were evaluated for two cases: Baseline Daylight (BD) and Summer Shaded (SS). For both cases, the data for a period of 6 days were used: SS data from June 23–28, 2022, and BD data from July 8–13, 2022. For both daylighting and glare, the hours of occupancy for the space were assumed to be from 8 A.M. to 5 P.M., following a schedule for a typical office.

3.1.3.1 Daylighting

The daylighting at each WPI sensor was calculated using the metric Useful Daylight Illuminance (UDI) [11]. UDI at each of the sensors was calculated as the percentage of illuminance values that fall between 100 and 2,000 lux during occupied hours. For the UDI metric, a higher number signifies more usable daylight throughout the day and is better for the occupant. UDI at different sensors for two cases, BD and SS, is provided in Figure 16 and Figure 17, respectively. Figure 16 shows that UDI in room 106 was slightly higher than 206, and the UDI in rooms 104 and 204 were similar (within 10% of each other). UDI was lower in the sensors near the south window in 106 and 206. Similarly, UDI in 104 and 204 was lower near the north window. The lower UDI in the sensors near the north and south windows is because the illuminance was higher than 2,000 lux at these sensors during occupied hours. Figure 17 shows a significant increase in UDI at sensors near the exterior windows from the use of cellular shades. The UDI at all of the sensors in the rooms with cellular shades (204 and 206) was greater than 85%. In the rooms without cellular shades (104 and 106), the UDI of the sensors near the window went as low as 3% for 104 and 6% for 106.

The time series of illuminance at sensor A1 for BD and SS for a period of 6 days for each case is provided in Figure 18. This time series is provided as a representative case to explain how the use of cellular shades affected illuminance at one of the sensor locations. Figure 18(a) shows that for BD, the illuminance was similar for rooms 106 and 206, and for SS, the illuminance for 206 was reduced to less than 2,000 lux (represented by the dashed red line in the figure) for most of the hours. Therefore, the UDI was enhanced compared with 106, where the number of occupied hours when the illuminance was higher than 2,000 lux was significant. A similar trend can be seen for 104 and 204 in Figure 18(b). This similarity shows that using cellular shades can make a significant improvement in useful daylight.

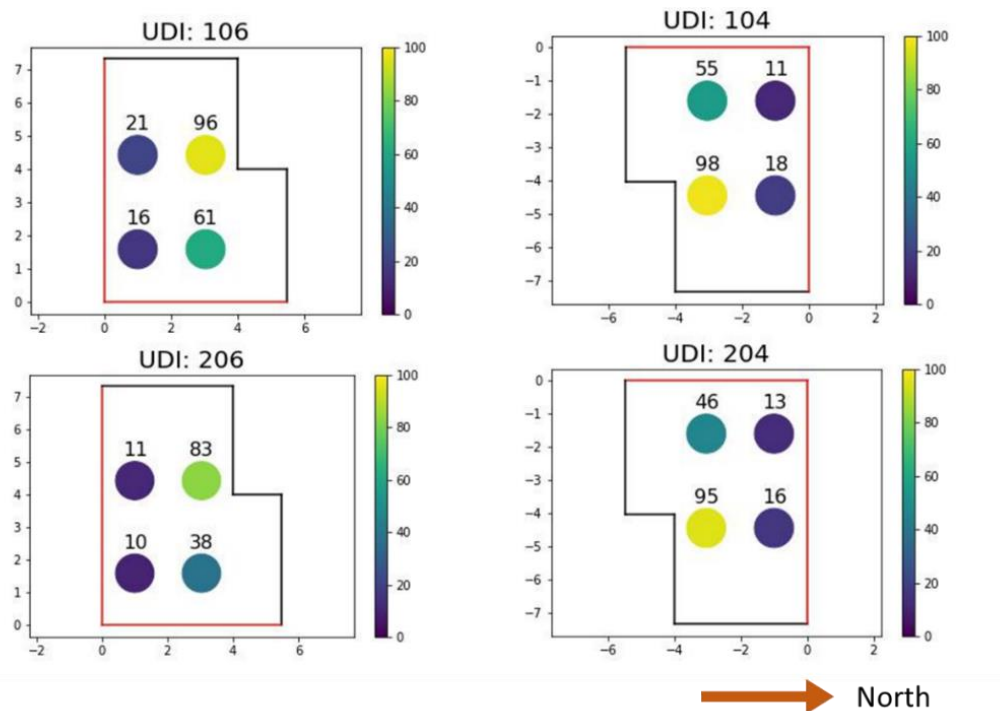


Figure 16. UDI at four different sensor locations for BD (all the windows are without any shading devices). Windows are located in the orientation with red-colored edges, and the sensors are directed toward the ceiling.

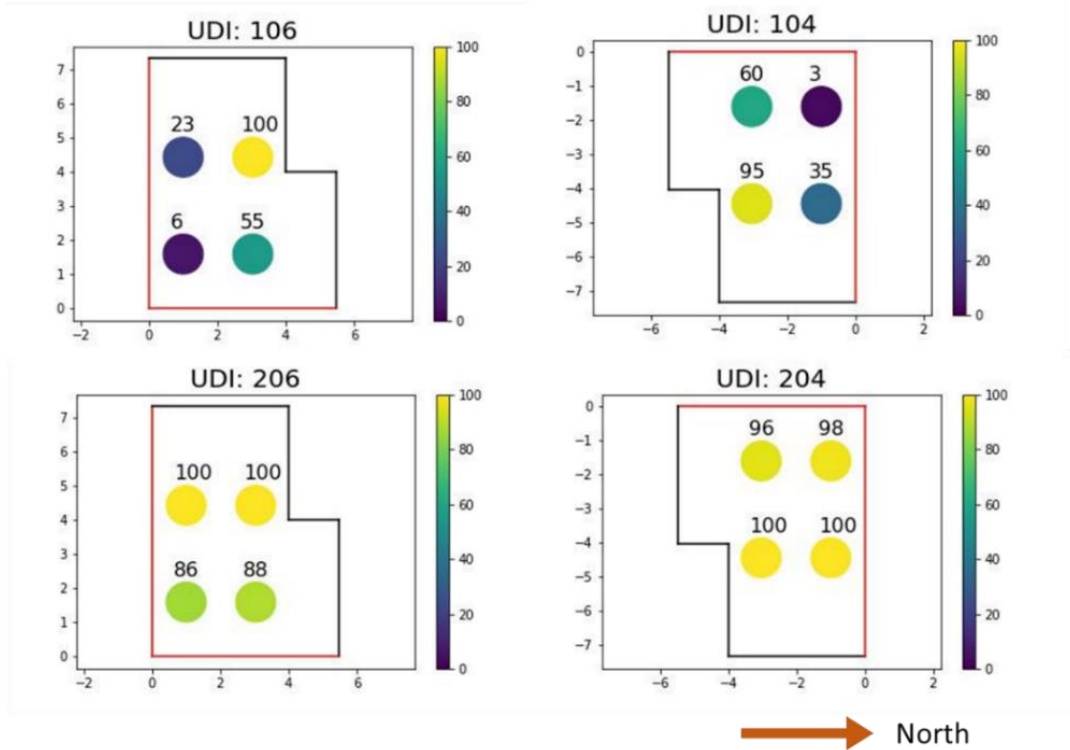


Figure 17. UDI at four different sensor locations for SS. Rooms 104 and 106 are without any shading devices, and windows in 204 and 206 are covered with cellular shades all day. Windows are located in the orientation with red-colored edges, and the sensors are directed toward the ceiling.

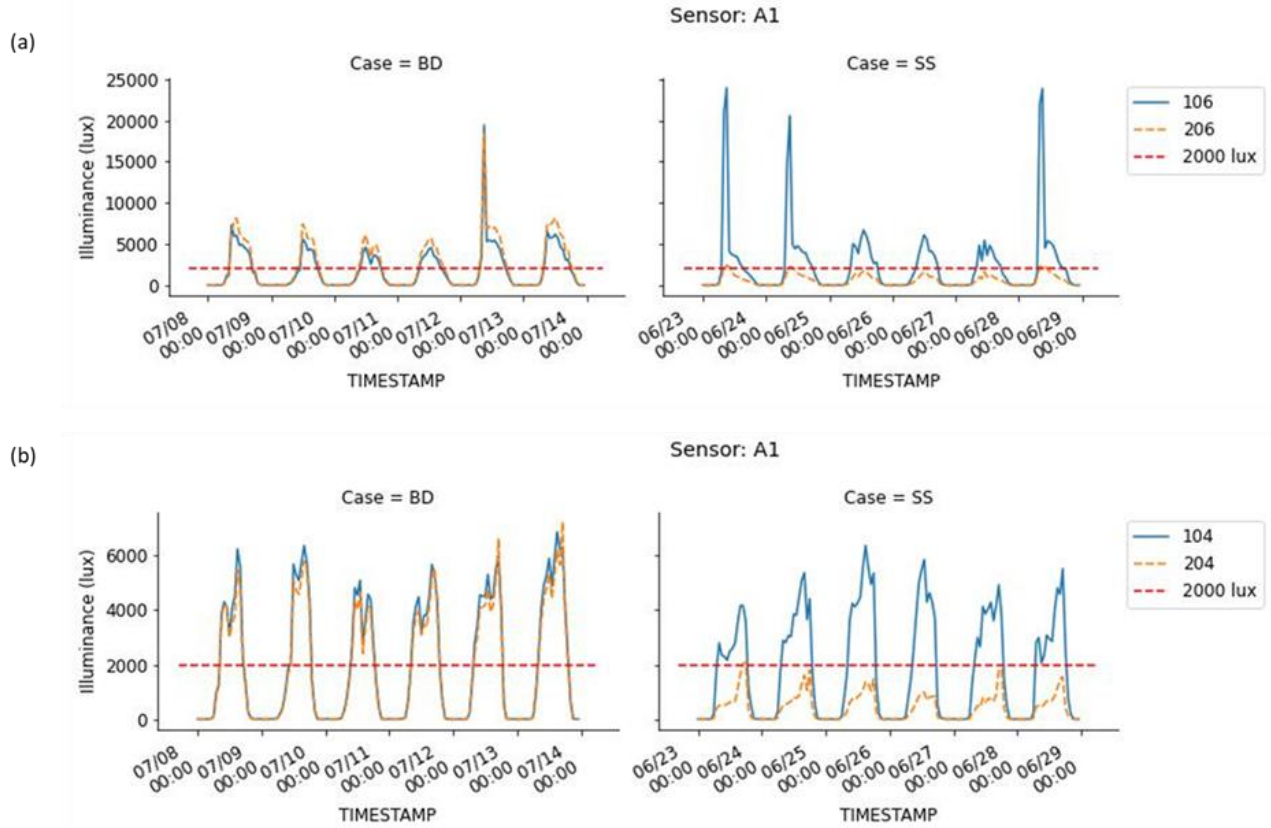


Figure 18. Illuminance at sensor A1 for BD and SS in rooms (a) 106 and 206 and (b) 104 and 204.

3.1.3.2 Glare

Glare was evaluated using two vertical illuminance sensors in the rooms. The data collected for vertical illuminance were used to evaluate the simplified daylight glare probabilities (DGPs) using Equation 1:

$$DGPs = (6.22 \times 10^{-5}) \times E_v + 0.184, \quad (1)$$

where E_v is the VI measurement using VI sensors.

A higher DGPs value indicates a higher likelihood of glare for the room occupant. Therefore, a lower DGPs is better for occupant comfort. The results for the DGPs of BD and SS are provided in Figure 19 and Figure 20, respectively, which show the percentage of the time when DGPs is above the threshold value of 0.35 ($DGPs_{>0.35}$). Figure 19 shows that $DGPs_{>0.35}$ in room 206 was slightly higher than that in room 106. Similarly, $DGPs_{>0.35}$ in 204 was higher than that in 104. The $DGPs_{>0.35}$ was higher than 50% in all the rooms and up to 85% in the south orientation in room 206.

After installing cellular shades in rooms 206 and 204, the $DGPs_{>0.35}$ were significantly reduced (see Figure 20). The $DGPs_{>0.35}$ equal 0 in these rooms at the south and north orientation after using cellular shades, and room 106 without any shade had $DGPs_{>0.35}$ of 91% of the time in the south orientation. The sensor facing the east and west orientation still had $DGPs_{>0.35}$ of 23% and 20%, respectively, after using cellular shades. These occurrences of higher $DGPs_{>0.35}$ in east and west orientations compared with the south orientation occur because of lower solar altitude in east and west orientations.

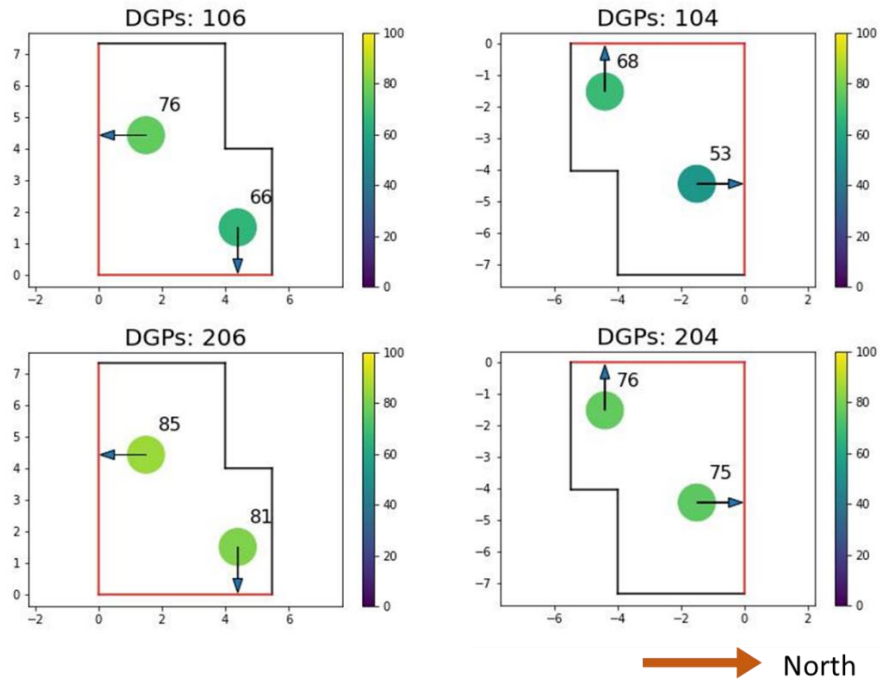


Figure 19. DGPs at two sensors for BD. Windows are located in the orientation with red colored edges, and the arrow represents the direction the sensor is facing.

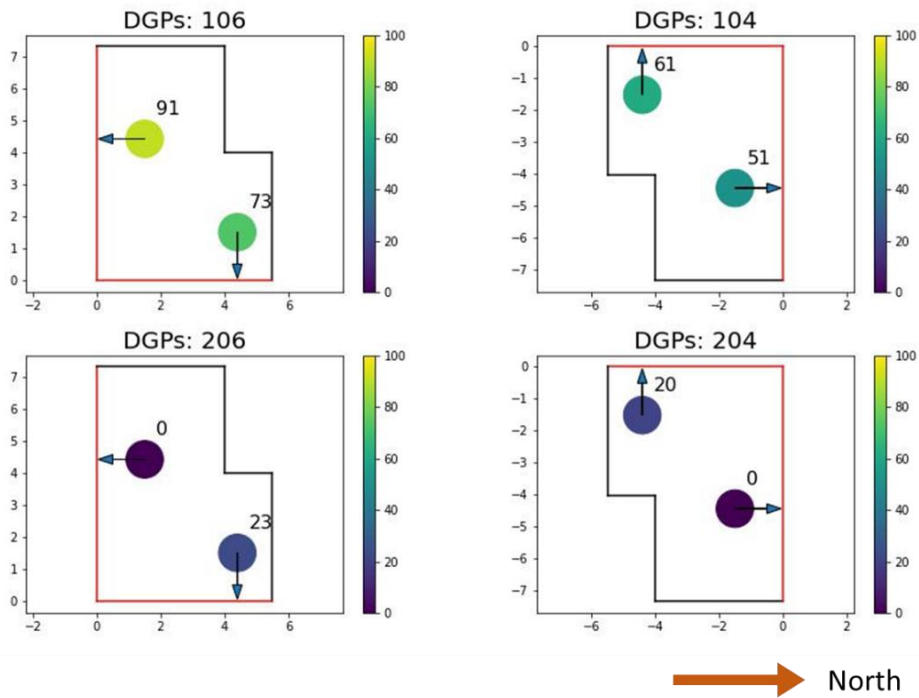


Figure 20. DGPs at two sensors for SS. Windows are located in the orientation with red colored edges, and the arrow represents the direction the sensor is facing.

3.2 ANNUAL SIMULATION

In this section, energy consumption and savings results are discussed for six cases for cooling, heating, and overall HVAC energy. The energy consumption results are presented in terms of energy use intensity (EUI) for cooling and heating in Figure 21 and Figure 22, respectively. Figure 21 shows that D22 had a higher reduction in cooling EUI compared to venetian blinds (Blinds) and roller shades (Shade). The EUI reduction in the Phoenix simulation was 13.8 kWh/m² for D22, which was 2.4 kWh/m² for Blinds and 6.1 kWh/m² for Shade. The difference in EUI between Low-e and D22 Low-e was 6.2 kWh/m², which shows the cooling energy savings potential of D22 if the baseline window was a Low-E window. Figure 22 shows the increase in EUI for Blinds and Shade compared with the Baseline, and energy savings was seen using D22. The heating site energy savings were 5.3 kWh/m² in Phoenix, 8.8 kWh/m² in Nashville, and 11.7 kWh/m² in Rochester.

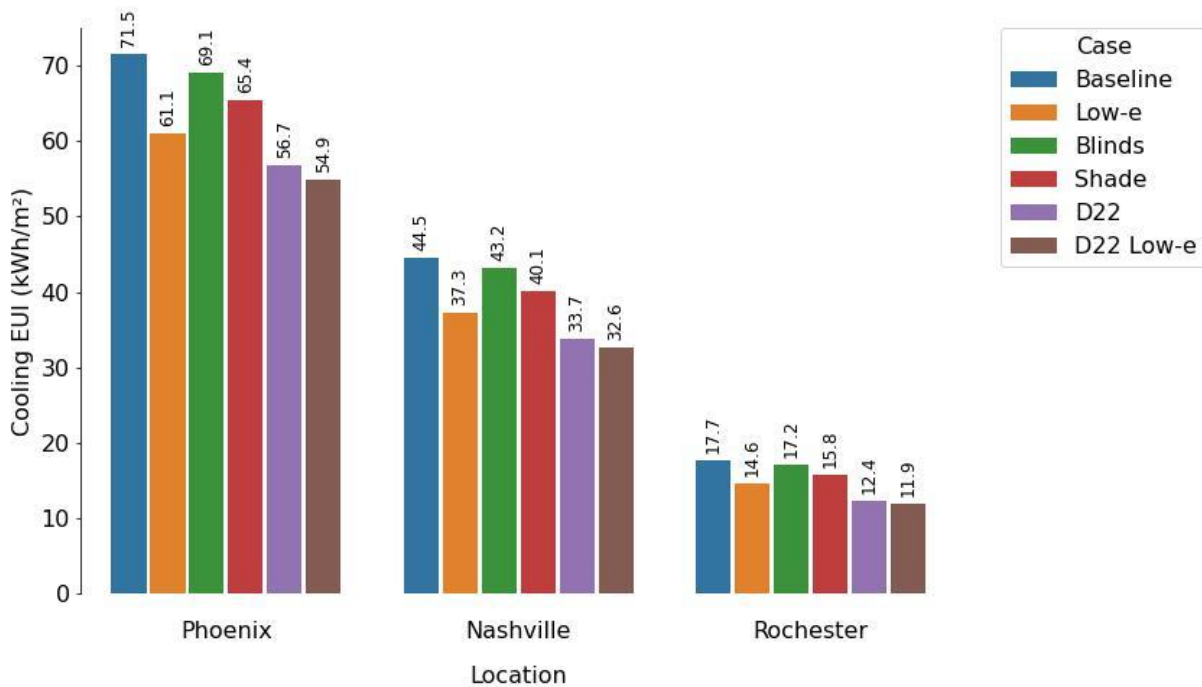


Figure 21. EUI for cooling for six cases and three locations.

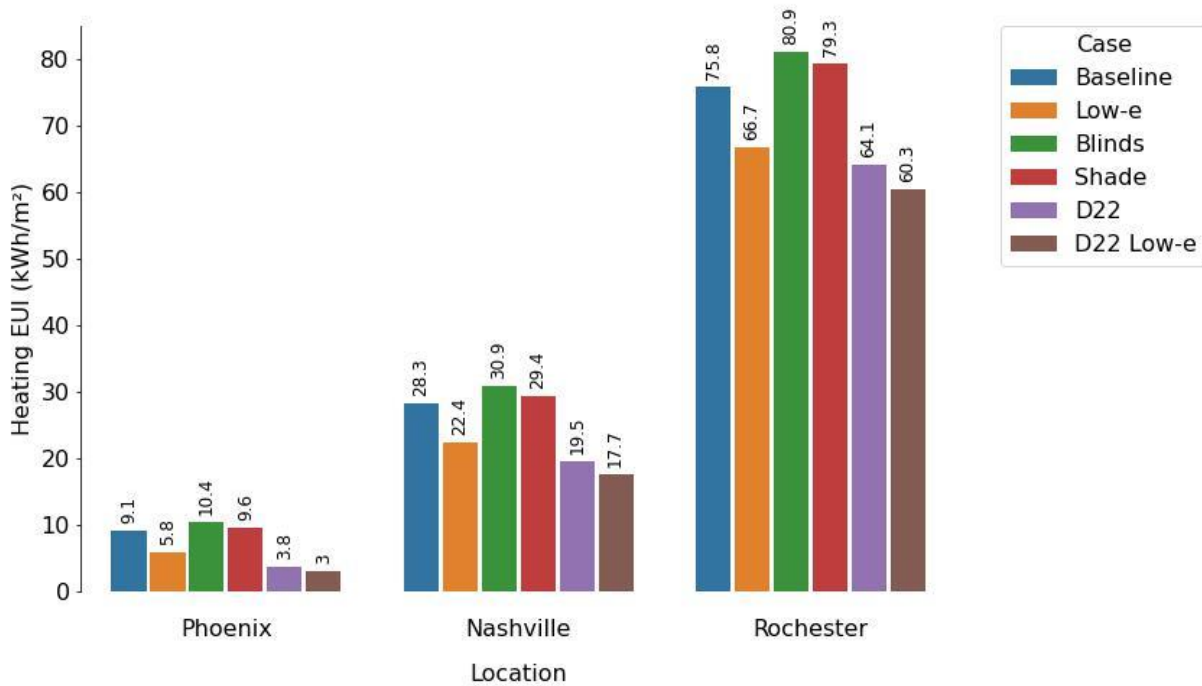


Figure 22. EUI for heating for six cases and three locations.

The percentage HVAC energy savings compared to the baseline case is shown in Figure 23. D22 cellular shades can save 19%–27% of HVAC energy compared with Baseline. Also, using generic venetian blinds (Blinds) can increase energy consumption in Rochester and Nashville. Generic roller shades (Shade) had a negative effect on Rochester and saved 7% energy consumption in Phoenix. The energy savings from using cellular shades (D22) was higher than Low-e, which had up to 18% energy savings. The combination of a Low-E window and D22 cellular shades (D22 Low-e) had the highest energy savings.

The energy savings from D22 Low-e were 10% higher than the energy savings from only Low-E, which shows the energy savings potential of cellular shades when installed on a Low-E window.

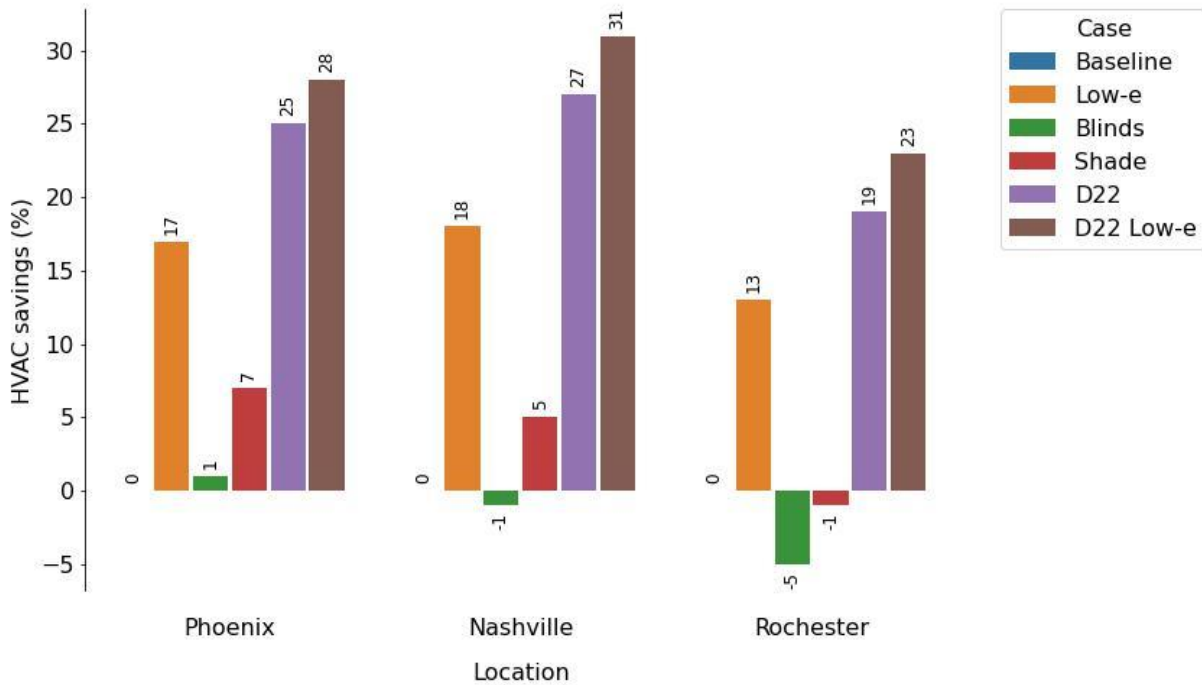


Figure 23. HVAC savings relative to baseline case for six cases and three locations.

4. CONCLUSIONS

Hunter Douglas D22 commercial cellular shades were experimentally tested in a light commercial building. The experimental testing provided results for energy usage, which was later used to calibrate an energy model, and for occupant comfort. Occupant comfort results showed enhancement in useful daylight and a reduction in glare. In one of the WPI sensors, UDI was higher by 95% in the room with cellular shades compared with a room with no shades. This was due to the room with no shades having illuminance values that exceeded the comfort level for a general office space of 100–2,000 lux. Similarly, a 91% lower DGPs was seen in a room with cellular shades with a VI sensor in the south orientation compared to a room with no shades. This lower DGPs means a much lower chance of glare and increased visual comfort for occupants in an office with shades. Another effect of cellular shades is that it helped maintain the MRT near the room temperature compared with a room without any shading device, resulting in increased thermal comfort for the occupants. All of these metrics were affected by window orientation and distance from the window.

The data from the experiment were also used to calibrate the baseline energy model and validate the cellular shades model. The cooling energy was within 5% of the measured data for the baseline calibrated model and 9.3% of the measured data for the model with cellular shades. Two different models for cellular shades were used to compare the results against the measured data. This comparison showed that the Simple model of a window was in very good agreement with measured data compared to the BSDF model, which is generally considered a better model for a complex fenestration system. The validated cellular shades Simple model was used for simulation in the US Department of Energy prototype building model. The results from the simulation showed that cellular shades can achieve 19%–27% energy savings at different locations in the United States. In addition to showing the energy saving potential of cellular

shades, the simulations also demonstrated that generic venetian blinds and roller shades can cause increased energy use in a light commercial building during heating seasons. These products may block beneficial passive heat gains during the day without improving the window system's thermal transmittance, which results in increased energy use at night.

Automation was able to help control window coverings throughout the day to take advantage of passive solar heating in the winter and block unwanted solar heat in the summer. A simple automation schedule was used for testing in the FRP based on window orientation and season. With this generalized automation schedule, rooms with south-facing windows (106 and 206) were still using cooling even in winter months. Room 206 with D22 shades saw increased cooling usage over room 106 with no shades. The automation schedule had the shades up during the day, which allowed both rooms to exceed the thermostat set point and require cooling, but room 206 would then close the shades in the late afternoon and likely trap heat in the room, thus needing less heating during the evening hours compared to room 106. Building-specific automation may help to provide opportunities for further energy savings compared with the generic schedule used in this study. Also, occupants in the buildings might override the automation schedule to take advantage of the daylighting and glare benefits of the cellular shades while also avoiding overheating in the winter months.

Through a combination of physical testing and simulation, this study has demonstrated that cellular shades show significant energy savings potential in commercial buildings with increased thermal and visual comfort.

5. REFERENCES

- [1] K.A. Cort, T.A. Ashley, J.A. McIntosh, C.E. Metzger Gp, S. G.P., N. Fernandez, S.N. Fernandez, Testing the Performance and Dynamic Control of Energy-Efficient Cellular Shades in the PNNL Lab Homes, PNNL Report No. 27663, Pacific Northwest Natl. Lab. (2018).
- [2] N.A. Kotey, J.L. Wright, C.S. Barnaby, M.R. Collins, Solar gain through windows with shading devices: Simulation versus measurement, ASHRAE Trans. 115 PART 2 (2009) 18–30.
- [3] DRI, Residential Windows and Window Coverings : A Detailed View of the Installed Base and User Behavior, 2013.
- [4] R. Hart, Numerical and experimental validation for the thermal transmittance of windows with cellular shades, Energy Build. 166 (2018) 358–371. <https://doi.org/10.1016/j.enbuild.2018.02.017>.
- [5] LBNL, WINDOW Technical Documentation, (2020). <https://windows.lbl.gov/tools/window/documentation> (accessed April 5, 2022).
- [6] Y. Tan, J. Peng, D.C. Curcija, R. Hart, J.C. Jonsson, S. Selkowitz, Parametric study of the impact of window attachments on air conditioning energy consumption, Sol. Energy. 202 (2020) 136–143. <https://doi.org/10.1016/j.solener.2020.03.096>.
- [7] N. Kunwar, M. Bhandari, D.C. Curcija, National energy savings potential of cellular shades: A measurement and simulation study, Build. Environ. 225 (2022) 109593. <https://doi.org/10.1016/j.buildenv.2022.109593>.
- [8] DOE, EnergyPlus, (2020). <https://energyplus.net/> (accessed February 4, 2020).
- [9] ASHRAE, Measurement of Energy, Demand, and Water Savings, 2014. www.ashrae.org/0Awww.ashrae.org/technology.
- [10] DOE, Commercial Prototype Building Models, (n.d.). https://www.energycodes.gov/development/commercial/prototype_models (accessed April 15, 2019).
- [11] A. Nabil, J. Mardaljevic, Useful daylight illuminances: A replacement for daylight factors, Energy Build. 38 (2006) 905–913. <https://doi.org/10.1016/j.enbuild.2006.03.013>.